J Mater Sci (2007) 42:4025–4030
DOI 10.1007/s10853-006-0381-4

Influence of nitriding gases on the growth of boron nitride nanotubes

Jun Yu · Bill C. P. Li · Jin Zou · Ying Chen

Received: 17 November 2005 / Accepted: 28 April 2006 / Published online: 31 January 2007

Abstract Boron nitride (BN) nanotubes of different sizes and tubular structures exhibit very different mechanical and chemical properties, as well as different applications. BN nanotubes of different sizes and nanostructures have been produced in different nitriding gases in a milling and annealing process, in which elemental boron powder was first milled in NH_3 for 150 h and subsequently annealed at 1,200 °C for 6 h. The influence of nitriding gases was investigated by using N_2, NH_3, N_2–H_2 mixture gases. A relatively slow nitriding reaction in NH_3 gas leaded to a 2D growth of BN (002) basal planes and the formation of thin BN nanotubes without the help of metal catalysts. Fast nitriding reactions occurred in N_2 or N_2–H_2 mixture gases, catalyzed by metal particles, resulted in 3D crystal growth and the formation of many large cylindrical and bamboo tubes.

Introduction

Boron nitride nanotubes (BNNTs) have many excellent properties as carbon nanotubes [1, 2], including some even better properties such as a stable insulator, a super-resistance to oxidation at high temperatures, and an excellent thermal conductivity [2, 3]. Several synthesis methods have been developed including electric arc-discharge [4], laser heating/ablation [5], milling-annealing [6], carbon nanotube substitution [7], and chemical vapor deposition [8]. Among them, the ball milling–annealing method has produced such large quantities that commercial BNNTs are available. In this method, boron powder is first ball milled in a high energetic mode at room temperature and subsequently annealed in a nitrogen-containing atmosphere [2]. The fundamental role of the high-energy ball milling treatment is creation of a precursor containing both nucleation structures and nanosized metal catalysts [9, 10]. BNNTs grow out from the precursor during the subsequent annealing process. BNNT growth depends strongly on the annealing temperatures and durations, indicating an in-situ nanotube growth during the nitriding reactions [11, 12]. Annealing atmospheres can also affect the nanotube growth as very different nanotubes have been produced from two different annealing gases (NH_3 and N_2) even with the same milled B sample. In the case of annealing in NH_3, only thin multiwalled BN nanotubes with diameter less than 20 nm are formed [12]; while annealing in N_2 gas produces the nanotubes with a very large diameter range from a few nanometers to more than 100 nm [9]. In this work, the influence of annealing gases on the nanotube growth is investigated by using N_2–H_2 mixture gases at different contents and the mechanisms of nanotube formation in different gases are discussed.

Experimental procedure

Amorphous boron powder (Sigma-Aldrich, 99%) was used as the starting material. High-energy ball milling

J. Yu · B. C. P. Li · Y. Chen (✉)
Department of Electronic Materials Engineering,
Research School of Physical Sciences and Engineering,
The Australian National University, Canberra, ACT 0200,
Australia
e-mail: ying.chen@anu.edu.au

J. Zou
School of Engineering and Centre for Microscopy and
Microanalysis, The University of Queensland, St. Lucia,
QLD 4072, Australia

treatment was conducted at room temperature using a high-energy rotating ball mill equipped with 4 hardened steel balls and a stainless steel cell [6]. The milling cell was loaded with several grams of the boron powder, and purged with NH_3 gas for several times. A starting pressure of 300 kPa of NH_3 gas was established prior to milling. The ball milling process lasted for 150 h at ambient temperature so that a large content of nitrogen gas was dissolved into the B powder through both gas absorption and a partial nitriding reaction induced under milling impacts [6, 9]. After the milling, the B samples were annealed for completion of the nitridation and nanotube growth in a horizontal alumina tube furnace up to 1,200 °C for several hours in different gases including N_2, N_2–H_2 mixture gases and NH_3 at the same flow rate of about 500 ml/min. BNNT samples were analyzed using X-ray powder diffraction (XRD) analysis with a Co radiation of $\lambda = 0.1789$ nm, field-emission scanning electronic microscopy (SEM) (Hitachi S4500, operated at 3 kV), and transmission electron microscopy (TEM) (Philips CM300, operated at 300 kV). A thin Pt-Au layer of about 3 nm was coated on the samples for SEM studies to reduce charging effect. The BNNT samples for TEM observation were deposited directed on holly carbon coated grids without any coating. The chemical contents were measured using both X-ray energy dispersive spectroscopy (EDS) in a JEOL (JSM6400) SEM equipment with an ultra-thin window for light element detection and energy filtered TEM (EFTEM) in a FEI F30 TEM equipped with a Gatan imaging filtering system.

Results and discussion

The SEM images in Fig. 1 show typical morphology of the BNNTs formed from the 150 h milled B samples after annealing at 1,200 °C for 6 h in different gases. Figure 1a shows BNNTs and some particles formed in pure N_2 gas. Both thin tubes (diameter less than 20 nm indicated by arrows) and thick nanotubes (diameter large than 20 nm) can be seen. The ratio of thin to thick tubes depends on annealing conditions [9]. Figure 1b and c show the BNNTs with a higher yield produced after annealing in N_2–5%H_2 (Fig. 1b) and N_2–15% H_2 (Fig. 1c) mixture gases, respectively. SEM images clearly indicate higher densities of nanotubes and the particle content, estimated from SEM images, is less than 10%. The inset in Fig. 1c shows both thin and thick nanotubes. The SEM image in Fig. 1d shows uniform thin nanotubes with a diameter less than 20 nm formed after the annealing in NH_3 gas, and no thick nanotubes were observed. Detailed SEM observation showed that the clusters observed are actually made of many thin nanotubes and thin layers [12]. The above SEM images clearly show a strong influence of the annealing atmosphere on the size and yield of BNNTs.

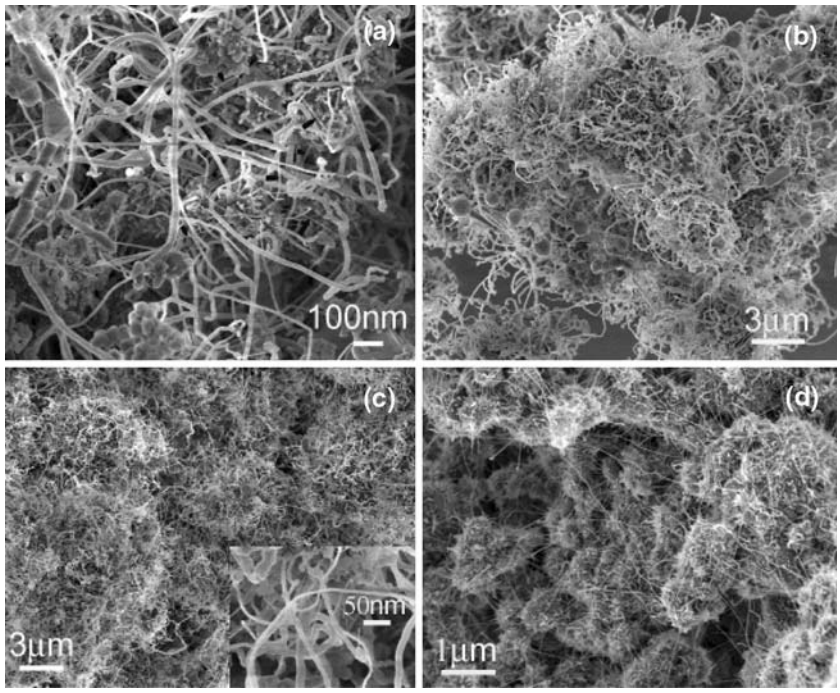

Fig. 1 SEM images of the typical morphology of the BNNTs annealed under different gases: (**a**) Pure N_2, (**b**) N_2–5% H_2, (**c**) N_2–15% H_2 (inset: higher magnification), and (**d**) NH_3

The size and structure of the BNNTs formed in different annealing gases were further investigated under TEM. The TEM image in Fig. 2a shows thin multiwalled BN nanotubes observed at the edge of a nanotube cluster. A typical straight cylindrical nanotube can be seen from the inserted high-magnification TEM image. The parallel fringes suggest a 4-layered cylindrical nanotube of a diameter about 7 nm. Most of the thin BNNTs have one end attached to the BN cluster, which may be due to the growth from the base clusters [13, 14]. Interestingly, no metal particle was found inside the nanotubes, although many Fe particles were observed in the samples. Nanotubes with larger diameters (large than 20 nm) or other structures such as bamboo and cone-like structures were not found. In contrast, the TEM images in Fig. 2b show different structures of the BNNTs formed in N_2 gas. Thick nanotubes with a bamboo structure and an outer diameter up to 120 nm were observed. The typical bamboo structure with repeated transverse layers is shown in the inserted image. The straight thin cylindrical BNNTs can also be observed as the arrow pointed. BNNTs formed in the two mixture gases have both thin and thick nanotubes, as well as cylindrical and bamboo type tubes. The TEM analysis confirmed the different size ranges observed under SEM, and revealed very different tubular structures.

The external diameter of BNNTs was measured on a large number (around 200) of the BNNTs observed on a number of SEM images taken under different magnifications. Although the Pt-Au thin coating adds additional 5 nm to the tube diameters, the size can still be compared between the samples as they were all coated under the same condition. In addition, TEM measurement of these samples confirmed the size range. The diameter distributions of the above four samples are compared in Fig. 3. The BNNTs formed in N_2, N_2–5% H_2, N_2–15% H_2 gases have a large diameter range from 6 to 100 nm as suggested by Fig. 3a–c. In contrast, the BNNTs produced in NH_3, as shown in Fig. 3d, have a much smaller external diameter and a very narrow diameter distribution from 5 to 20 nm. The average diameter of the BNNTs, calculated from the diameter distributions, decreases from about 50 to 8 nm with increasing H content from 0% (pure N_2) to 75% (NH_3). These results indicate

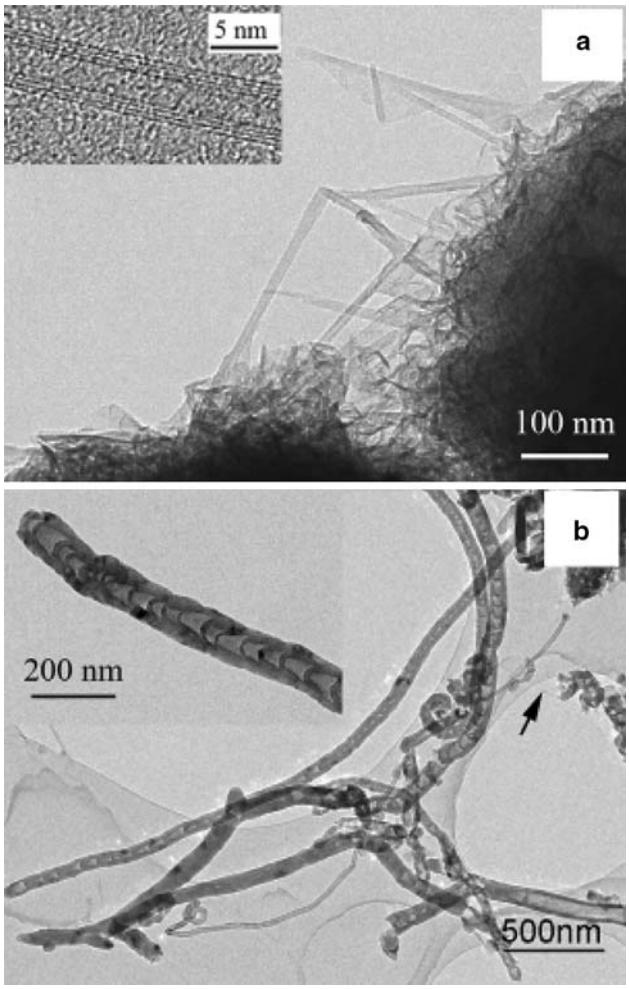

Fig. 2 TEM images of BNNTs annealed in different gases: (**a**) NH_3: the typical straight cylindrical BNNTs have a diameter about 7 nm. (Inset: the HRTEM image of a 4-layered cylindrical nanotube); (**b**) N_2: the bamboo structures of an outer diameter from 20 to 120 nm. (Inset: the typical bamboo structure with the transverse layers)

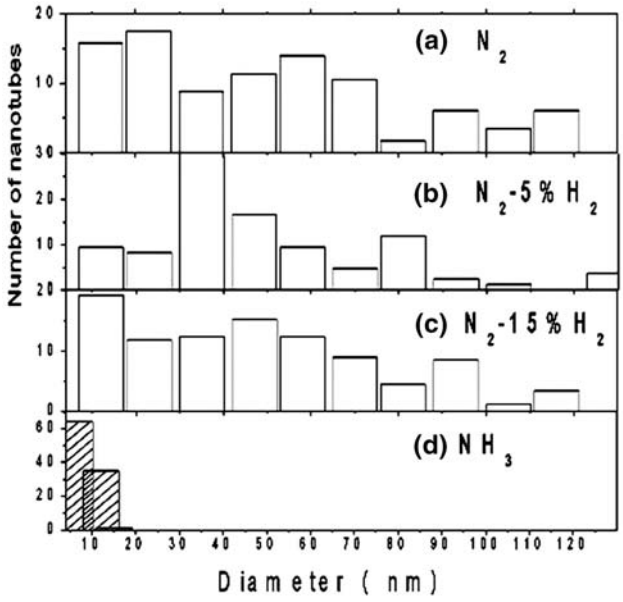

Fig. 3 External diameter distributions of BNNTs measured on a large number of BNNTs observed from the SEM images

that hydrogen gas might affect the nitriding reactions and enhance the formation of the nanotubes with a small diameter. Similar effect has been previously observed in the case of carbon nanotube growth [15]. The diameter distributions of BNNTs can be changed by varying annealing temperatures and times [9, 11].

The BN structure formed during the annealing was examined using XRD analysis. The XRD spectra taken from the samples heated in N_2–15% H_2, N_2 and NH_3 gases are shown in Fig. 4. The BN phase can be identified by the presence of the BN (002) and (100) diffraction peaks at 31.2 and 48.7 degrees. The sharp and pronounced (002) diffraction peaks in Fig. 4a and b suggest a large size of BN crystallites (thick (002) layers) formed in N_2 and N_2–15% H_2 gases. The appearance of the (100) peak indicates the formation of bulk hexagonal BN phase with certain orientations between the basal planes, which is consistent with the observation of thick and multiwalled cylindrical and bamboo tubes under TEM [16]. In contrast, in the case of NH_3 gas, the relatively weak and broadened (002) peak (Fig. 4c) indicates the formation of thin layers of the (002) planes and a possible 2D growth with the formation of many (002) basal planes. The (100) peak is difficult to be determined because of the overlap with board Fe peaks. Because the intensity of the (001) peak should be 15% of that of the (002) peak, the (001) peak might not exist or is very weak too. Single or thin (002) layers were observed under both SEM and TEM (Figs. 1d and 3a). The significant differences in the shape and intensity of the BN diffraction peaks in the XRD patterns suggest different nitriding reactions occurred during the annealing in different gases. The pronounced α-Fe diffraction peaks in Fig. 4a and b indicate a large number of active catalyst Fe particles, which are reduced from stainless steel Fe(Cr, C) during nitriding reactions. The steel particles came from the milling balls and container as milling contamination but have a positive catalyst role in nanotube formation. The Fe catalyst role can be seen clearly from the elemental mapping of EFTEM shown in Fig. 5. The bright field (BF) image shows a dark particle capsulated inside a tube. B and N maps indicate clearly that the tube is made of BN. The Fe and Cr maps suggest the dark particle contains dominant Fe and some Cr. The C map shows almost absence of C at the particle area and a low level of C on the surface of the tube possibly due to sample contamination. These EFTEM analyses reveal the formation of thick BN nanotubes with the help of Fe(Cr) particle in N_2 and the mixture gas. Such catalytic effect was not observed in the

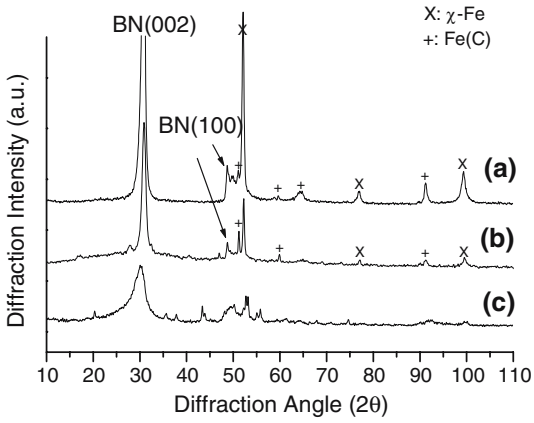

Fig. 4 XRD spectra taken from the samples heated in different gases: (**a**) N_2–15% H_2; (**b**) N_2, and (**c**) NH_3

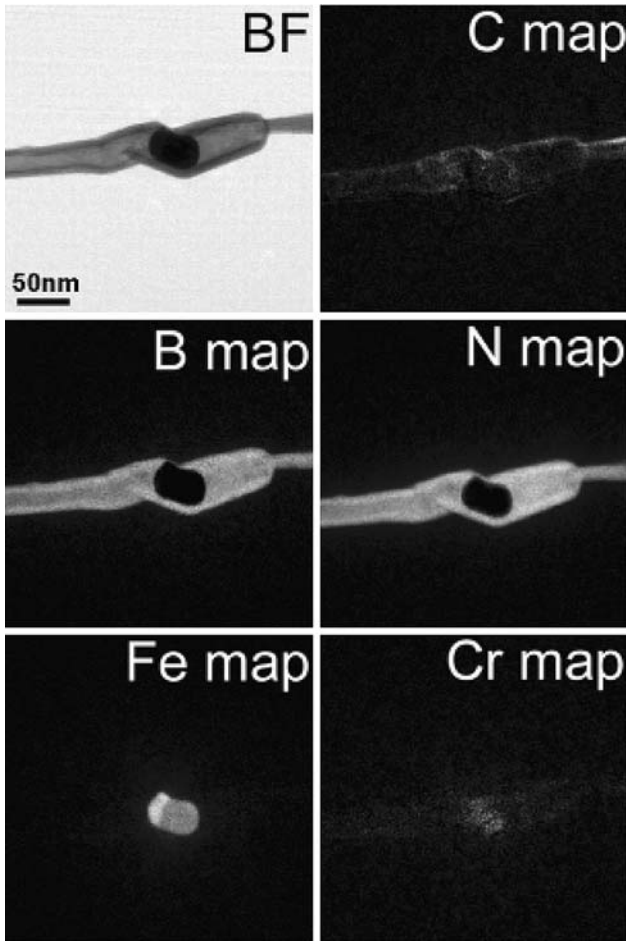

Fig. 5 EELS elemental mapping of a BN nanotube containing a metal particle inside. Table Content Graphic: The size and structure of the BN nanotubes synthesized using milling and annealing method can be controlled by using different nitriding gases, which lead to different nitriding reactions and metal catalytic effects. The elemental mapping of energy-filtered TEM images showing a BN nanotube containing a Fe–Cr catalyst particle

sample heated in NH_3. Therefore, the structures and sizes of the BNNTs could be determined by the formation of the BN phases produced from the nitriding reactions between the milled B and the N containing gases as elemental B must be first converted to the BN phase before forming tubular structures.

Two different nitriding reactions occurred during annealing under different gases. In the case of N_2 gas, the decomposition of molecular nitrogen into atomic N is an equilibrium reaction. The nitriding process is driven by the reaction potential, which is determined by the partial pressure of nitrogen (P_N). P_N can be reduced by the use of H_2 commonly to promote the reaction. In nitrogen and hydrogen mixture gases, hydrogen dilutes the P_N, leading to faster nitridation of B in pure N_2. Indeed, EDS analysis revealed a higher N content (N/B = 0.87) in B samples heated in mixture gases compared with the sample heated in N_2 (N/B = 0.72), which is also consistent to the XRD results. In the case of ammonia gas, more H_2 gas is released from the decomposition reaction, resulting in the lowest nitrogen partial pressure P_N. Further, nitrogen and hydrogen decomposed from NH_3 are more reactive. Therefore, the nitriding reaction in NH_3 gas should proceed faster than that in N_2 and the mixture gases. However, EDS analysis reveals that the sample heated in NH_3 has a lower N content (N/B = 0.66) compared with those heated in N_2 and mixture gases. The weak BN diffraction peaks in the XRD patterns (Fig. 4c) also suggest a possible partial nitridation. Two possible reasons may be responsible to the relatively lower nitridation degree in NH_3 gas. The first one is that metal catalysts did not act. The starting milled B sample contains same amount of Fe/Cr particles (about 1 at%), these metal particles acted as the catalysts and produced thick nanotubes with or without bamboo structures in N_2 and N_2–H_2 mixture gases, but did not work in the NH_3 atmosphere. The second reason might be the gas flow rate. The reaction rate is affected by the equilibrium NH_3–H_2–N_2 gas mixture, which is controlled by the NH_3 flow rate. Under the same flow rate, the ammonia gas provides only half of N to the nitriding reaction compared with N_2 gas. In-situ investigation of the nitriding reactions in different atmospheres and flow rates with the formation of BN nanotubes has been conducted using thermal gravimetric analyzers (TGA). Detailed results will be published later.

In N_2 and N_2–H_2 gases, when the nitriding reaction proceeds too fast, a rapid growth of BN structures and even three-dimensional growth occurred as indicated by XRD measurement. Furthermore, Fe particles have played important catalytic role in the formation of thick BN nanotubes and particles; while in NH_3 gas, relatively slow nitriding reaction produces only (002) layers and thus avoids the formation of large tubes and particles. In addition, Fe particles did not play the catalytic role, maybe because more reactive N and H atoms decomposed from NH_3 can react directly with B so that metal catalysts are not needed [17], thick bamboo tubes are thus not formed. Other hydrogen containing gases such as H_2O vapor can help the formation of BN nanotubes as reported by Ma et al. [18]. It has also been found that thin C and BN nanotubes can be formed in the ball milled C and B without the help of metal catalysts [10, 14] and the catalyst-free BNNTs have been also produced using a different method [19].

Conclusions

BNNTs of different sizes and structures were produced from the same ball milled B sample after annealing in different gases including N_2, N_2–H_2 mixture gases and NH_3. Annealing in NH_3 gas produces thin multiwalled cylindrical nanotubes with a diameter less than 10 nm. Annealing in N_2 and N_2–H_2 mixture gases produces both thin cylindrical tubes and thick bamboo nanotubes of a diameter up to 120 nm. A slow nitriding reaction in NH_3 gas appears to lead to a 2D growth of (002) basal planes. Thin BN nanotubes are therefore formed without the help of metal catalysts. A fast nitriding reaction in N_2 and N_2–H_2 mixture gases produces 3D BN phases and large bamboo tubes with the help of metal catalysts. The nanotubes with different sizes and structures offer different properties and meet different requirements from various applications.

Acknowledgements Authors would like to thank Dr John Fitzgerald and the staff at the Electron Microscopy Unit for their help in microscopy analysis, and Professor L.T. Chadderton for the fruitful discussion. This work is supported partially by one Discovery research grant awarded by the Australian Research Council

References

1. Loiseau A, Willaime F, Demoncy N, Schramchenko N, Hug G, Colliex C, Pascard H (1998) Carbon 36:743
2. Chen Y, Williams JS (2005) In: Schultz MJ (ed) Nanoengineering of structural, functional and smart materials, CRC Press LLC, p 167
3. Chen Y, Zou J, Campbell SJ, LeCaer G (2004) Appl Phys Lett 84:2430
4. Chopra NG, Luyken RJ, Cherrey K, Crespi VH, Cohen ML, Louie SG, Zettl A (1995) Science 269:966

5. Golberg D, Bando Y, Eremets M, Takemura K, Kurashima K, Yusa H (1996) Appl Phys Lett 69:2045
6. Chen Y, Fitz Gerald JD, Williams JS, Bulcock S (1999) Chem Phys Lett 299:260
7. Golberg D, Han W, Bando Y, Bourgeois L, Kurashima K, Sato T (1999) J Appl Phys 86:2364
8. Lourie OR, Jones CR, Bartlett BM, Gibbons PC, Ruoff RS, Buhro WE (2000) Chem Mater 12:1808
9. Chen Y, Conway M, Williams JS, Zou J (2002) J Mater Res 17:1896
10. Chadderton LT, Chen Y (1999) Phys Lett A 263:401
11. Fitz Gerald JD, Chen Y, Conway MJ (2003) Appl Phys A Mater Sci Process 76:107
12. Yu J, Chen Y, Wuhrer R, Liu ZW, Ringer SP (2005) Chem Mater 17:5172
13. Chen Y, Chadderton LT, Williams JS, Fitz Gerald JD (2000) Metastab Mech Alloyed Nanocryst Mater 343–3(Pts 1 and 2):63
14. Chen Y, Conway MJ, Fitz Gerald JD, Williams JS, Chadderton LT (2004) Carbon 42:1543
15. Choi YC, Bae DJ, Lee YH, Lee BS, Han IT, Choi WB, Lee NS, Kim JM (2000) Synth Met 108:159
16. Golberg D, Bando Y, Bourgeois L, Kurashima K, Sato T (2000) Appl Phys Lett 77:1979
17. Jacob KT, Verman R, Mallya RM (2002) J Mater Sci 37:4465
18. Ma R, Bando Y, Sato T (2002) Japanese society of electron microscopy, p S259
19. Lee RS, Gavillet J, de la Chapelle ML, Loiseau A, Cochon JL, Pigache D, Thibault J, Willaime F (2001) Phys Rev B 64:121405